Machine learning based model to diagnose obstructive coronary artery disease using calcium scoring, PET imaging, and clinical data

J. A. van Dalen, PhD,[a] S. S. Koenders, MSc,[b,e] R. J. Metselaar, MSc,[b,e] B. N. Vendel, MD,[b] D. J. Slotman, MSc,[c] M. Mouden, MD, PhD,[d] C. H. Slump, PhD,[e] and J. D. van Dijk, MSc, PhD, MBA[b]

[a] Department of Medical Physics, Isala Hospital, Zwolle, The Netherlands
[b] Department of Nuclear Medicine, Isala Hospital, Zwolle, The Netherlands
[c] Department of Radiology, Isala Hospital, Zwolle, The Netherlands
[d] Department of Cardiology, Isala Hospital, Zwolle, The Netherlands
[e] Technical Medical Centre, University of Twente, Enschede, The Netherlands

Received Jul 7, 2022; accepted Nov 15, 2022
doi:10.1007/s12350-022-03166-3

Introduction. **Accurate risk stratification in patients with suspected stable coronary artery disease is essential for choosing an appropriate treatment strategy. Our aim was to develop and validate a machine learning (ML) based model to diagnose obstructive CAD (oCAD).**

Method. **We retrospectively have included 1007 patients without a prior history of CAD who underwent CT-based calcium scoring (CACS) and a Rubidium-82 PET scan. The entire dataset was split 4:1 into a training and test dataset. An ML model was developed on the training set using fivefold stratified cross-validation. The test dataset was used to compare the performance of expert readers to the model. The primary endpoint was oCAD on invasive coronary angiography (ICA).**

Results. **ROC curve analysis showed an AUC of 0.92 (95% CI 0.90-0.94) for the training dataset and 0.89 (95% CI 0.84-0.93) for the test dataset. The ML model showed no significant differences as compared to the expert readers ($p \geq 0.03$) in accuracy (89% vs. 88%), sensitivity (68% vs. 69%), and specificity (92% vs. 90%).**

Conclusion. **The ML model resulted in a similar diagnostic performance as compared to expert readers, and may be deployed as a risk stratification tool for obstructive CAD. This study showed that utilization of ML is promising in the diagnosis of obstructive CAD. (J Nucl Cardiol 2023)**

Key Words: Machine learning • PET myocardial perfusion imaging • Coronary artery disease

Supplementary Information The online version contains supplementary material available at https://doi.org/10.1007/s12350-022-03166-3.

The authors of this article have provided a PowerPoint file, available for download at SpringerLink, which summarises the contents of the paper and is free for re-use at meetings and presentations. Search for the article DOI on SpringerLink.com.

Reprint requests: J. A. van Dalen, PhD, Department of Medical Physics, Isala Hospital, PO Box 104008000 GK Zwolle, The Netherlands; *jo.van.dalen@isala.nl*

J Nucl Cardiol
1071-3581/$34.00

Published online: 09 January 2023

Abbreviations	
CACS	Calcium scoring
CT	Computed tomography
ICA	Invasive coronary angiography
MBF	Myocardial blood flow
MFR	Myocardial flow reserve
ML	Machine learning
MPI	Myocardial perfusion imaging
Ocad	Obstructive coronary artery disease
PET	Positron emission tomography
Rb-82	Rubidium-82

INTRODUCTION

Invasive coronary angiography (ICA) in combination with functional flow measurements is an important procedure in diagnosing obstructive coronary artery disease (oCAD). However, it is associated with inherent risks of serious complications and accompanied by considerable costs, relatively high radiation exposure, and patient discomfort.[1,2] In patients with low to intermediate pre-test likelihood for oCAD, non-invasive imaging, such as computed tomography (CT) based calcium scoring (CACS), CT coronary angiography (CCTA), and cardiac positron emission tomography (PET) is recommended as gatekeeper for ICA.[1,3,4]

After non-invasive imaging, cardiologists combine the imaging data, clinical data, and type of complaints to estimate a post-test likelihood and, if needed, determine a specific treatment strategy. Typically, they include classical risk factors for oCAD such as age, body mass index, smoking, hypertension, cholesterol, diabetes, medical history and family history, and medication usage. In the end, this may include tens of different features which makes the cardiologist's ability to interpret and integrate all these data into one post-test likelihood not straight forward. Artificial intelligence (AI) applications can help to improve diagnosis of patients with oCAD by combining all available information.[5,6] These applications may reduce costs, save time, can help training or starting physicians and increase diagnostic performance. In particular, machine learning (ML) models have been shown suitable to assess many features and are capable of modeling complex non-linear relations between these features, to finally result in an accurate diagnosis and to guide physicians in the treatment strategy to choose.[7,8]

In order to integrate AI applications into clinical practice it is appropriate that these applications result in a diagnostic performance at least equal to that of an experienced physician. Previous studies have shown the potential of integrating imaging derived features with clinical data in ML-based risk prediction models.[7,8] To our knowledge, a study applying ML to predict oCAD based on clinical data, CACS, and PET imaging, has not been performed yet.

Our aim was to develop and validate a ML-based model to diagnose oCAD in patients without prior history of CAD, based on clinical data, medication, and imaging data, including CT-based CACS and Rubidium-82 (Rb-82) PET. In addition, we compared the performance of this ML model to that of expert imaging physicians.

MATERIALS AND METHODS

Study population

We retrospectively have included a consecutive cohort of 1007 patients who underwent CT-based CACS and rest and regadenoson-induced stress Rb-82 PET (Discovery 690, GE Healthcare) between 1 May 2017 and 1 February 2019. All included patients had no prior history of CAD which was defined as prior myocardial infarction, percutaneous coronary intervention (PCI) or coronary artery bypass grafting (CABG). Information about the patients' history, patients' characteristics, and clinical data were obtained by review of medical records. As this study was retrospective, approval by the medical ethics committee was therefore not required according to Dutch law. Nevertheless, all patients provided written informed consent for the use of their data for research purposes.

Image acquisition and reconstruction

Prior to myocardial perfusion imaging (MPI), a low-dose CT scan was acquired during free-breathing to provide an attenuation map of the chest. This scan was made using 0.8 s rotation time, pitch of 0.97, collimation of 32 × 0.625 mm, tube voltage of 120 kV, and a tube current of 10 mA. Images were reconstructed using a matrix of 512 × 512 and a 5 mm slice thickness. Next, 740 MBq Rb-82 was administered intravenously with a flow rate of 50 mL/min using a Sr-82/Rb-82 generator (CardioGen-82, Bracco Diagnostics Inc.). Ten minutes after the first elution, we induced pharmacological stress by administrating 400 μg (5 mL) of Regadenoson over 10 s. After a 5 mL saline flush (NaCl 0.9%), we administered a second dose of 740 MBq Rb-82. Seven-minute PET list-mode acquisitions were acquired after both Rb-82 administrations. Attenuation correction was applied to all data on the PET system after manual rigid registration of CT and PET data.

CT-based CACS scans were performed using a 64-slice CT scanner (Light-Speed VCT XT, GE Healthcare). An unenhanced ECG-gated scan was obtained prospectively, triggered at 75% of the R–R interval by using the following scanning parameters: 2.5 mm slice thickness; 330 ms gantry rotation time; tube voltage of 120 kV; and a tube current of 125-250 mA, depending on patient's size.

Static and ECG-gated rest and stress PET images (Discovery 690, GE Healthcare) were obtained from data acquired from 2:30 to 7:00 min after Rb-82 administration. The voxel size was $3.3 \times 3.3 \times 3.3$ mm^3. The dynamic PET datasets were reconstructed using 26 time-frames (12×5 s, 6×10 s, 4×20 s, and 4×40 s) with default settings as recommended by the manufacturer using 3D iterative reconstruction using 2 iterations and 24 subsets, while correcting for decay, attenuation, scatter and random coincidences, and dead time effects. Neither time-of-flight information nor resolution modeling was used for reconstruction of the dynamic PET datasets.

Data processing

CACS was obtained per vessel (left anterior descending (LAD), left circumflex (LCX), and right coronary artery (RCA)) according to the standard Agatston criteria.[9] All acquired PET data were post-processed using Corridor4DM software (Invia medical imaging solutions, v2015.02.64) to obtain the left-ventricle ejection fraction (EF) and semi-quantitative PET parameters including summed stress score (SSS) and summed difference score (SDS). The reconstructed dynamic images were used in combination with the one-tissue compartment model of Lortie et al. to calculate the myocardial blood flow (MBF),[10] as also described previously.[11] The MBF was calculated for the myocardium as a whole and for the LAD, LCX, and RCA territories, for both stress and rest. The MFR was calculated by dividing the stress MBF by the rest MBF. The dynamic images were visually inspected for the presence of myocardial creep and manually corrected if necessary. Rest MBF was calculated without rate-pressure product correction.

To possibly further improve the diagnostic accuracy of the MBF measurements, we also calculated the myocardial perfusion entropy (MPE). MPE can be interpreted as the amount of disorder between the 17-segmental MBF values and can possibly better discriminate ischemic from non-ischemic areas as compared to global or regional MBF values.[12] MPE was calculated using Shannon's equation for entropy[13] with the 17-segmental MFR values as input.[12]

Follow-up

A reference standard was used to determine the diagnostic value of a ML-based model in the diagnosis of oCAD. As reference standard, we classified patients as having oCAD if follow-up included a conclusive invasive coronary angiography (ICA) for CAD defined by an intermediate stenosis with a fractional flow reserve < 0.8, or a $> 70\%$ stenosis in the LAD, LCX or RCA, or a $> 50\%$ stenosis in the left main coronary artery.[14]

Machine learning

For the selection of the machine learning model for this study we compared the diagnostic performance of the following models using test data that were not used for training of the models (as explained further below): Least Absolute Shrinkage and Selection Operator (LASSO), Logistic Regression, Support Vector Machine (SVM), and the eXtreme Gradient Boosting (XGBoost) algorithm. Finally, we continued with XGBoost (library v1.4.2) to diagnose oCAD in patients without prior history of CAD, based on clinical data, medication and imaging data, including CAC-score and Rb-82 PET.[15] The XGBoost model implements the gradient boosting decision tree model and was carried out in Python from the Scikit-Learn library (v0.24.2) for binary classification of the presence of oCAD.[16] The dataset was randomly split into a training and test set with a 4:1 ratio as illustrated in Figure 1, stratified by occurrence of obstructive events, so that both the training and test set had a comparable prevalence of oCAD. Each patient was characterized by an array of features, including (semi-)quantitative SDS, SSS, MBF and MFR measurements and CACS, and various other clinical features which are shown in Table 1. All features except MBF, MFR, CACS, age, resting heart rate, and body mass index (BMI), were transformed to dichotomous variables. The remaining continuous variables of the training dataset were normalized such that the mean value was 0 and standard deviation was 1. Next, the mean and standard deviation of the training dataset were used to normalize the test dataset.

Model development and feature importance

The XGBoost model was optimized with the training dataset, using hyperparameter optimization via grid search in combination with fivefold stratified cross-validation as shown in Figure 1. Additionally, the feature importance was extracted from the model. The feature ranking is based on the number of times a feature

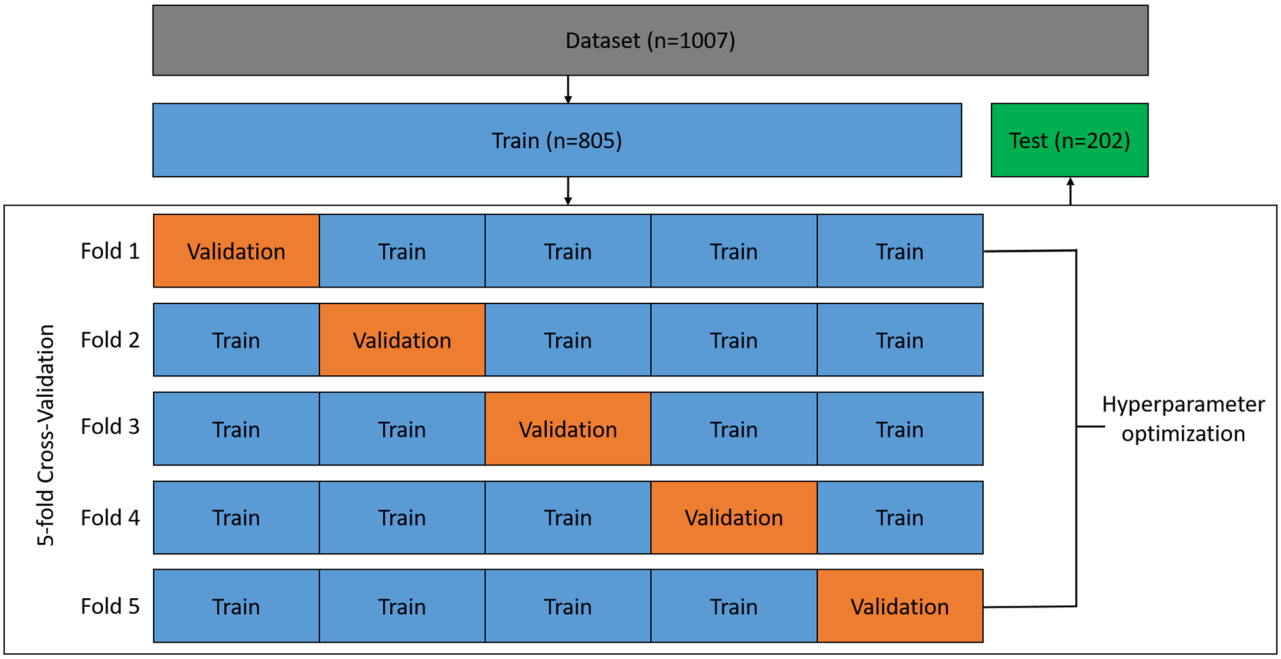

Figure 1. Visualization of the cross-validation procedure of the development of the XGBoost model. The entire dataset is initially split 4:1 into a training and test dataset. The training set is used to optimize hyperparameters via cross-validation. The test dataset is used in to evaluate the performance in an independent patient population.

appeared (F-score) in decision trees within the model. The model with the highest F1-score was evaluated on the test dataset.

Model and readers' performance

Two expert readers, a cardiologist and nuclear medicine physician, assessed the clinical data, CACS, and the Rb-82 PET data for each patient. After the expert readers reached consensus of possible or definite defect, based on all these data, patients were categorized as having oCAD. Otherwise, patients were categorized as non-oCAD. To assess the value of the XGBoost model in the detection of oCAD, the predictive performance of the model was compared to that of the expert readers. The reference for both the expert readers and the XGBoost model was oCAD on ICA.

Statistical analysis

Statistical analysis was performed using IBM SPSS (IBM SPSS Statistics for Windows, Version 26.0. Armonk, NY: IBM Corp). Differences in patient characteristics between the training and test dataset were evaluated using Student's *t*-test, or Mann–Whitney *U* test, when appropriate. Following a Bonferroni correction for the comparisons of the basic characteristics between the training and test dataset, the level of statistical significance was set to 0.05/48 = 0.001 for all statistical analyses.

Furthermore, we computed the accuracy, sensitivity, and specificity, achieved by the expert readers, for detecting oCAD. Next, the area under the receiver operating curve (AUC) was computed for the XGBoost model for both the training and test dataset. From the receiver operating curve (ROC) of the training dataset we determined two different model thresholds to discriminate between non-oCAD and oCAD. The first being the model threshold that resulted in a similar sensitivity as compared to the sensitivity obtained by the expert readers ($threshold_{sens}$). The second being the model threshold that resulted in a similar specificity as compared to the specificity obtained by the expert readers ($threshold_{spec}$). Next, the performance metrics (accuracy, sensitivity, and specificity) were calculated on both the training and test dataset. The performance metrics of the XGBoost model was compared to those of the readers using McNemar's test. Following a Bonferroni correction for the comparisons of the expert readers to the two model thresholds applied to both datasets, the level of statistical significance was set to 0.05/4 = 0.0125.

RESULTS

Data that were used as input features for the ML model and follow-up data for the training and test set are summarized in Table 1. Of the included 1007 patients,

Table 1. Summary of data that were used as input features for the XGBoost model and follow-up data of both the training and test dataset

	Training set (n = 805)	Test set (n = 202)	*p* values
Input features			
Age (years)	66 ± 11	66 ± 11	0.54
Male (%)	50	52	0.77
Length (cm)	174 ± 10	174 ± 11	0.54
Weight (kg)	89 ± 20	89 ± 20	0.80
BMI	25.6 ± 5.2	25.6 ± 5.1	0.93
Pulse (beats/min)	70 ± 14	70 ± 11	0.56
Creatinine serum (μmol/L)	97 ± 76	90 ± 41	0.19
Smoking never (%)	40	39	0.70
Smoking ever (%)	47	47	0.84
Smoking present (%)	13	15	0.38
Diabetes mellitus (%)	20	18	0.49
Hypercholesterolemia * (%)	41	41	0.89
Hypertension (%)	62	61	0.80
Family history (%)	51	47	0.25
Medical history (%)	20	27	0.02
COPD (%)	12	16	0.09
CVA (%)	9	13	0.12
Medication usage (%)	94	97	0.12
Aspirin (%)	28	27	0.78
Clopidogrel (%)	4	5	0.82
Acenocoumerol (%)	9	11	0.40
Beta blockage (%)	54	62	0.03
Ace/AII inhibitor (%)	41	45	0.34
Ca-channel blocker (%)	24	18	0.08
Statin (%)	43	47	0.33
Diuretic (%)	29	36	0.06
Total CAC-score	449 ± 771	505 ± 845	0.36
LM CAC-score	21 ± 55	24 ± 67	0.49
LAD CAC-score	187 ± 298	194 ± 258	0.77
LCX CAC-score	88 ± 210	77 ± 186	0.48
RCA CAC-score	153 ± 360	200 ± 442	0.16
PET SSS	6 ± 7	6 ± 6	0.87
PET SDS	2 ± 4	3 ± 4	0.24
EF stress	64 ± 12	63 ± 13	0.06
EF rest	59 ± 12	58 ± 12	0.23
Global stress MBF (mL/min/g)	2.5 ± 0.7	2.5 ± 0.8	0.30
Global rest MBF (mL/min/g)	1.1 ± 0.3	1.1 ± 0.3	0.75
Global MFR	2.5 ± 0.6	2.4 ± 0.6	0.36
LAD stress MBF (mL/min/g)	2.5 ± 0.7	2.5 ± 0.7	0.27
LAD rest MBF (mL/min/g)	1.1 ± 0.3	1.1 ± 0.3	0.61
LAD MFR	2.4 ± 0.6	2.4 ± 0.6	0.45
LCX stress MBF (mL/min/g)	2.5 ± 0.7	2.4 ± 0.8	0.32
LCX rest MBF (mL/min/g)	1.1 ± 0.3	1.1 ± 0.3	0.80
LCX MFR	2.4 ± 0.7	2.4 ± 0.7	0.38
RCA stress MBF (mL/min/g)	2.7 ± 0.8	2.6 ± 0.9	0.46
RCA rest MBF (mL/min/g)	1.1 ± 0.4	1.1 ± 0.4	0.99
RCA MFR	2.6 ± 0.7	2.5 ± 0.8	0.36

Table 1 continued

	Training set (n = 805)	Test set (n = 202)	*p* values
MPE	1.3 ± 0.7	1.2 ± 0.7	0.16
Follow-up data			
Obstructive CAD (%)	11	11	0.95
All cause death (%)	2.6	2.5	0.92
Time to obstructive CAD (months)	1 [0–5.5]	1 [0–3]	0.23
Event < 90 days after scan (%)	8	8	0.82

*Hypercholesterolemia was defined as a known history of dyslipidemia (total cholesterol > 200 mg/dl or LDL cholesterol levels > 130 mg/dl) or treatment with cholesterol-lowering medication
Data are presented as mean ± SD, median [interquartile range] or percentage;
The *p* values are given for either the χ^2 test, t-test or Mann–Whitney *U* test

111 (11%) patients were classified as having oCAD during follow-up. An additional 26 (3%) patients died during follow-up. The median follow-up time was 1.8 years. The minimum follow-up time was 1 year while the longest follow-up time was 2.7 years. Most cases of oCAD occurred within 90 days after the PET scan (early revascularization), 67% in the training dataset and 73% in the test dataset, respectively. No significant differences were found in patient characteristics between the training and test datasets ($p > 0.02$).

Machine learning

We tested multiple ML models to compare the performance: LASSO (AUC of 0.84), Logistic Regression (AUC of 0.84), and SVM (AUC of 0.75), but the XGBoost algorithm (AUC of 0.89, see further below) performed best. Features were ranked in order of importance for the XGBoost model for oCAD. The top 10 predictors for the XGBoost model consisted of CACS and PET-derived features, as shown in Figure 2. The summed difference score (SDS) was the most important feature with an F-score of 44. Features with a feature importance of less than one and therefore with little to non-predictive value for oCAD were length, family history, medical history, COPD, past CVA, hypertension, and present smoking. In addition, all prescribed medication categories were found to hold little to non-predictive value (F-score ≤ 1).

Using oCAD on ICA as reference ROC curve analysis showed an AUC of 0.92 for the training dataset and 0.89 for the test dataset, respectively, as shown in Figure 3. The expert readers achieved an accuracy of 88% (sensitivity 69% and specificity 90%) for the detection of oCAD as shown in Table 2 and Figure 4. No significant ($p \geq 0.03$) differences in accuracies (89% and 82%), sensitivities (68% and 73%), and specificities (92% and 83%) were found for the XGBoost model on the test data as compared to the expert readers, using either $\text{threshold}_{\text{sens}}$ or $\text{threshold}_{\text{spec}}$, respectively.

To put our results into perspective we conducted ROC analyses based on the SSS alone, stress MBF (global) alone, and MFR (global) alone. The corresponding ROCs for the test dataset are shown in the supplementary material. With AUCs ranging from 0.71 to 0.76, the performance of these single PET-based features is inferior to that of the ML model (AUC of 0.89) that includes multiple features.

DISCUSSION

In this study we have developed and tested an XGBoost model to diagnose patients with oCAD, using clinical data, CACS, and Rb-82 PET imaging data. The ML model resulted in a high AUC (0.89) on the test data and showed a comparable performance to that of the expert readers. In clinical practice, such a model can serve as a post-test likelihood test for oCAD and be used to improve risk stratification and thereby decisions in low to intermediate risk patients regarding further testing or therapies.

We were also able to identify the most important predictors of oCAD via feature importance ranking of the XGBoost model. PET derived (semi-)quantitative values including SDS, SSS, MBF, and MFR, as well as CACS were much stronger predictors as compared to classical risk factors such as smoking and hypertension. The importance of PET and CACS features is not unexpected, since these are well established as independent and complementary predictors.[17,18] Furthermore, the creatinine serum level was ranked as a relatively strong predictor. This may be explained by the

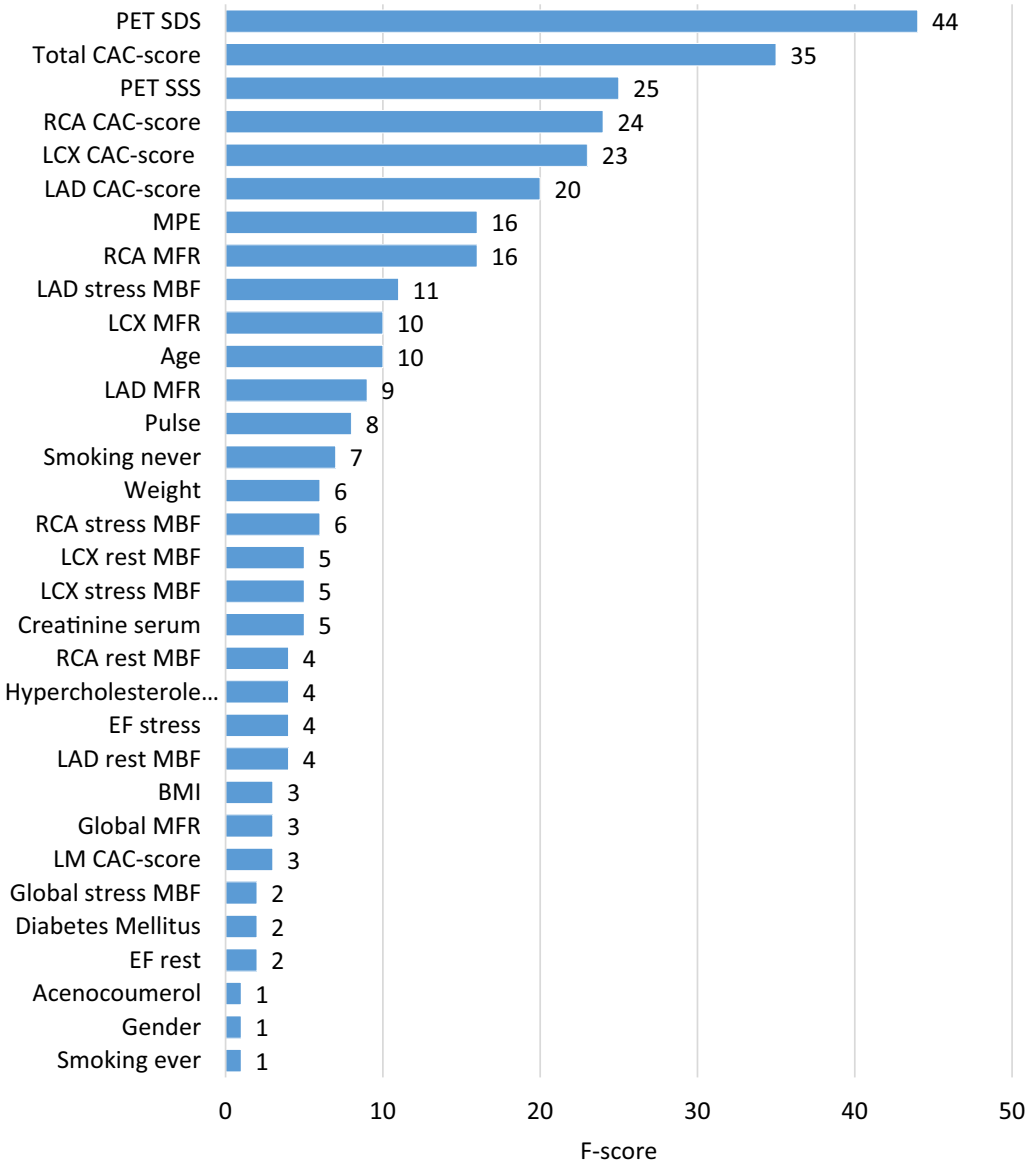

Figure 2. Feature importance ranking of features with F-scores > 0 of the XGBoost model to detect obstructive CAD. The F-score was calculated by the improvement in accuracy brought by a feature to the branches it is on. Features with low importance can be interpreted as weak predictors for obstructive CAD. BMI body mass index; CAC-score coronary artery calcium score; EF ejection fraction; LAD left anterior descending artery; LCX left circumflex; LM left main artery; MBF myocardial blood flow; MFR myocardial flow reserve; MPE myocardial perfusion entropy; RCA right coronary artery; SDS summed difference score; SSS summed stress score.

experience that renal dysfunction increases the likelihood of CAD and has a negative impact on the prognosis.[19]

There are several studies on the performance of models on the basis of clinical data, CACS and/or nuclear imaging data (SPECT or PET), but none of them combined all these features into one model. In 2013, Arsanjani et al.[8] already showed that ML significantly improved diagnostic performance of MPI with SPECT by computational integration of quantitative perfusion and clinical data to the level rivaling expert analysis. Fathala et al.[3] showed that the addition of CACS to MPI with PET may help in the detection of subclinical CAD, especially in patients with unknown history of CAD. Al'Aref et al. compared the performance of a ML model alone, ML model with CACS, CAD consortium clinical

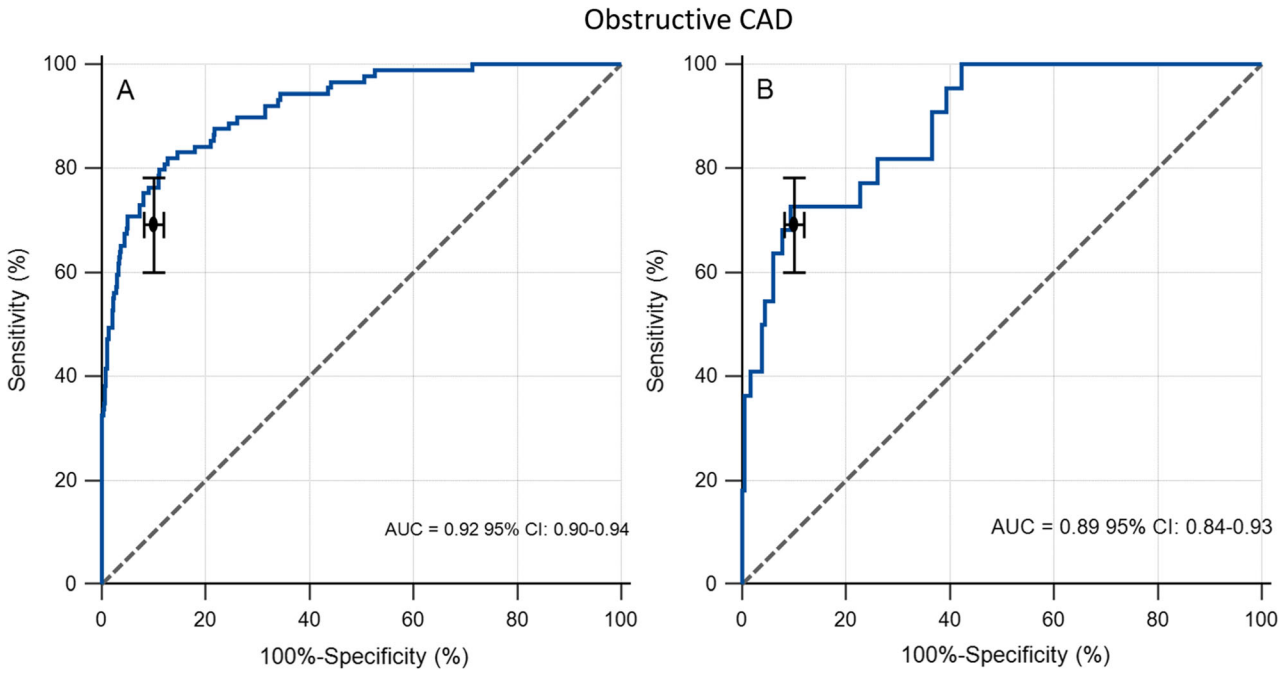

Figure 3. ROC curve of the XGBoost model for detection of obstructive CAD on the (A) training (n = 805) and (B) test (n = 202) dataset. The sensitivity and specificity of the expert readers, is plotted (black dot) with corresponding 95% confidence intervals.

Table 2. Diagnostic performance of expert readers and the ML model for the detection of obstructive CAD. By definition the 69% sensitivity and the 90% specificity of the training data are equal to those of the expert readers

	Expert readers (reference)	Training data		Test data	
		$Threshold_{sens}$	$Threshold_{spec}$	$Threshold_{sens}$	$Threshold_{spec}$
Accuracy	88%	92%*	88%	89%	82%
Sensitivity	69%	69%	76%	68%	73%
Specificity	90%	95%*	90%	92%	83%

*$p < 0.013$

score, CAD consortium score with CACS and updated Diamon-Forrester score to predict the presence of oCAD on CCTA.[20] They concluded that ML using clinical data in addition to CACS can accurately estimate the pretest likelihood of oCAD. ML with CACS produced the best performance with an AUC of 0.87. In our study all relevant data (clinical, CACS, and PET) were combined and the ML model resulted in a performance with an AUC of 0.89 on the test data using oCAD on ICA as reference.

This study has several limitations. First, we used data of one hospital which makes generalizability to other centers not straight forward. Although most input parameters of the ML model are or can be standardized (clinical information and CACS), MBF measurements based on PET are generally not standardized among different centers and depend on several technical aspects such as reconstructions settings and post-processing software.[21-24] Still, for each center it is possible and even recommendable to retrain and test the ML model to their unique patient data. Although this will take effort, it will lead to center-specific optimized hyperparameter values and hence likely to the best diagnostic performance.

Second, we classified patients as having oCAD if follow-up included a conclusive invasive coronary angiography (ICA) for oCAD[7] during follow-up. Inherently, we might have missed patients with oCAD as not

Figure 4. Column chart showing the performance of detecting obstructive CAD on the test dataset (n = 202) by expert physicians (blue bars) and the XGBoost model using threshold$_{sens}$ (orange) and threshold$_{spec}$ (gray). No significant differences were observed in detecting obstructive CAD between the experts and the XGBoost model using either threshold$_{sens}$ or threshold$_{spec}$.

all were referred for ICA. This bias may lead to underestimation of the positive cases.

Third, CACS was obtained using the Agatston method, which has limitations,[25,26] e.g., it assumes that calcium should be upwardly weighted with increased calcium density in the CT scan and it does not account for the regional distribution within the coronary tree. However, its use is current practice in most hospitals and therefore we used it in our study. Moreover, if we would have used a different method to obtain the CACS, we do not expect that it would change our conclusion. Both the ML model and the expert readers used the same CACS.

Fourth, the number of patients included was relatively low. In particular we had an imbalanced dataset as the number of patients who were classified as having oCAD was only 111 (11%) of the total population. Furthermore, only 20% of the patients were included in the test dataset, which resulted in performance metrics with relatively large confidence intervals. This only allowed us to demonstrate that the ML model performance did not significantly differ from the readers' performance. Using a larger database or using more advanced artificial intelligence algorithms might possibly show a superiority of the ML model. Moreover, the retrospective study design may have led to some bias in our study population, since we only included patients who were referred to our institution for both CACS and Rb-82 PET imaging.

Finally, the ML model was only trained and tested on patients without prior history of CAD. Therefore, the ML model might not be generalizable to patients with a prior history of CAD. However, by retraining the model on data from a different patient population we expect that a high diagnostic performance can be obtained as well.

NEW KNOWLEDGE GAINED

The XGBoost model derived in this study is an objective classification approach for identifying patients with oCAD and led to a similar performance compared to that of expert physicians. It is therefore expected to facilitate the detection of oCAD, risk stratification, and finally optimize patient-specific treatment when using it as a post-test likelihood tool. As this technological innovation provides automated interpretation of data it might also help physicians in training.

CONCLUSION

We have developed and validated a machine learning model to diagnose obstructive CAD in patients without prior history of CAD, based on clinical risk factors, medication, and imaging data, including CACS and Rb-82 PET. It resulted in similar performance as compared to the performance of experts imaging physicians. Therefore, utilization of such a model is promising in the diagnosis of obstructive CAD. It may be used for risk stratification for obstructive CAD and eventually for guiding further patient treatment.

DISCLOSURES

The authors declare that they have no conflict of interest.

References

1. Montalescot G, Sechtem U, Achenbach S, Andreotti F, Arden C, Budaj A. 2013 ESC guidelines on the management of stable coronary artery disease: The task force on the management of stable coronary artery disease of the european society of cardiology. Eur Heart J 2013;34:2949-3003.
2. Carpeggiani C, Picano E, Brambilla M, Michelassi C, Knuuti J, Kauffman P, et al. Variability of radiation doses of cardiac diagnostic imaging tests: The RADIO-EVINCI study (RADIationdOse subproject of the EVINCI study). BMC Cardiovasc Disord 2017;17:1-8.
3. Fathala A, Aboulkheir M, Shoukri MM, Alsergani H. Diagnostic accuracy of 13N-ammonia myocardial perfusion imaging with PET-CT in the detection of coronary artery disease. Cardiovasc Diagn Ther 2019;9:35.
4. van Diemen PA, Schumacher SP, Driessen RS, Bom MJ, Stuijfzand WJ, Everaars H, et al. Coronary computed tomography

angiography and [15 O] H 2 O positron emission tomography perfusion imaging for the assessment of coronary artery disease. Neth Hear J 2020;28:57-65.
5. Slart RH, Williams MC, Juarez-Orozco LE, Rischpler C, Dweck MR, Glaudemans AW, et al. Position paper of the EACVI and EANM on artificial intelligence applications in multimodality cardiovascular imaging using SPECT/CT, PET/CT, and cardiac CT. Eur J Nucl Med Mol Imaging 2021;48:1399-413.
6. Chan S, Bailey J, Ros PR. Artificial intelligence in radiology: Summary of the AUR academic radiology and industry leaders roundtable. Acad Radiol 2020;27:117-20.
7. Juarez-Orozco LE, Knol RJ, Sanchez-Catasus CA, Martinez-Manzanera O, Van der Zant, Friso M, Knuuti J. Machine learning in the integration of simple variables for identifying patients with myocardial ischemia. J Nucl Cardiol 2020;27:147-55
8. Arsanjani R, Xu Y, Dey D, Vahistha V, Shalev A, Nakanishi R, et al. Improved accuracy of myocardial perfusion SPECT for detection of coronary artery disease by machine learning in a large population. J Nucl Cardiol 2013;20:553-62.
9. Agatston AS, Janowitz WR, Hildner FJ, Zusmer NR, Viamonte M, Detrano R. Quantification of coronary artery calcium using ultrafast computed tomography. J Am Coll Cardiol 1990;15:827-32.
10. Lortie M, Beanlands R, Yoshinaga K, Klein R, DaSilva J, deKemp R. Quantification of myocardial blood flow with 82Rb dynamic PET imaging. Eur J Nucl Med Mol Imaging 2007;34:1765-74. https://doi.org/10.1007/s00259-007-0478-2.
11. Koenders SS, van Dijk JD, Jager PL, Ottervanger JP, Slump CH, van Dalen JA. Impact of regadenoson-induced myocardial creep on dynamic rubidium-82 PET myocardial blood flow quantification. J Nucl Cardiol 2019;26:719-28.
12. Van Dalen J, Koenders SS, Vendel BN, Jager PL, Van Dijk JD. Entropy-based myocardial blood flow measurements using PET: A way to improve reproducibility. Eur Heart J Cardiovasc Imaging. 2021;22:jeab111.6. https://doi.org/10.1093/ehjci/jeab111.066.
13. Shannon CE. A mathematical theory of communication. Bell Syst Tech J 1948;27:379-656. https://doi.org/10.1002/j.1538-7305.1948.tb01338.x.
14. Yokota S, Mouden M, Ottervanger JP, Engbers E, Jager PL, Timmer JR, et al. Coronary calcium score influences referral for invasive coronary angiography after normal myocardial perfusion SPECT. J Nucl Cardiol 2019;26:602-12.
15. Chen T, Guestrin C. Xgboost: A scalable tree boosting system. Proc 22nd ACM SIGKDD International Conference on Knowledge Discovery and Data Mining. 2016:785-94.
16. Pedregosa F, Varoquaux G, Gramfort A, Michel V, Thirion B, Grisel O, et al. Scikit-learn: Machine learning in python. JMLR 2011;12:2825-30.
17. Neves PO, Andrade J, Monção H. Coronary artery calcium score: Current status. Radiol Bras 2017;50:182-9.
18. Ziadi M, deKemp R, Williams K, Guo A, Renaud J, Chow B, et al. Does quantification of myocardial flow reserve using rubidium-82 positron emission tomography facilitate detection of multivessel coronary artery disease? J Nucl Cardiol 2012;19:670-80.
19. Murthy V, Bateman T, Beanlands R, Berman D, Borges-Neto S, Chareonthaitawee P, et al. Clinical quantification of myocardial blood flow using PET: Joint position paper of the SNMMI cardiovascular council and the ASNC. J Nucl Cardiol 2018;25:269-97.
20. Al'Aref SJ, Maliakal G, Singh G, van Rosendael AR, Ma X, Xu Z, et al. Machine learning of clinical variables and coronary artery calcium scoring for the prediction of obstructive coronary artery disease on coronary computed tomography angiography: Analysis from the CONFIRM registry. Eur Heart J. 2020;41:359-67.
21. Koenders SS, van Dijk JD, Jager PL, Mouden M, Tegelaar AG, Slump CH, et al. Effect of temporal sampling protocols on myocardial blood flow measurements using rubidium-82 PET. J Nucl Cardiol. 2021. https://doi.org/10.1007/s12350-021-02555-4.
22. Murthy VL, Lee BC, Sitek A, Naya M, Moody J, Polavarapu V, et al. Comparison and prognostic validation of multiple methods of quantification of myocardial blood flow with 82Rb PET. J Nucl Med 2014;55:1952-8.
23. Tahari AK, Lee A, Rajaram M, Fukushima K, Lodge MA, Lee BC, et al. Absolute myocardial flow quantification with (82)rb PET/CT: Comparison of different software packages and methods. Eur J Nucl Med Mol Imaging 2014;41:126-35.
24. Armstrong I, Tonge C, Arumugam P. Impact of point spread function modeling and time-of-flight on myocardial blood flow and myocardial flow reserve measurements for rubidium-82 cardiac PET. J Nucl Cardiol 2014;21:467-74.
25. Shea S, Navas-Acien A, Shimbo D, Brown ER, Budoff M, et al. Spatially weighted coronary artery calcium score and coronary heart disease events in the multi-ethnic study of atherosclerosis. Circ Cardiovasc Imaging 2021;14:1.
26. Blaha MJ, Mortensen MB, Kianoush S, Tota-Maharaj R, Cainzos-Achirica M. Coronary artery calcium scoring. JACC Cardiovasc Imaging 2017;10:823-937.